

A Numerical Study of the Agulhas Retroflexion: The Role of Bottom Topography

RICARDO P. MATANO

College of Oceanic and Atmospheric Sciences, Oregon State University, Corvallis, Oregon

(Manuscript received 8 November 1995, in final form 10 April 1996)

ABSTRACT

The oceanic circulation near the eastern margin of the African continent is dominated by the poleward flow of the Agulhas Current. The Agulhas Current separates from the African coast near the southern tip of the continent, makes an abrupt turn to the east (known as the Agulhas Retroflexion), and flows into the Indian Ocean as a meandering jet called the Agulhas return current. The object of this study is to investigate possible causes for the Agulhas Retroflexion. A series of process-oriented experiments are conducted with the Princeton ocean model, a primitive equation numerical model in sigma coordinates. The model is started from rest, forced at its surface with different wind stress distributions, and run until dynamical equilibria are reached, after which the steady states of the model are analyzed. In these experiments, the effects of inertia, wind stress distribution, and realistic bottom topography on the Agulhas Retroflexion are analyzed. The results of these experiments indicate that bottom topography, rather than current inertia, is the main cause of the Agulhas Retroflexion.

1. Introduction

The oceanic circulation near the eastern margin of the African continent is dominated by the poleward flow of the Agulhas Current, the western boundary current of the southern Indian Ocean. The Agulhas Current derives most of its water from flow through the Mozambique Channel (Harris 1972), from southward flow to the east of Madagascar (Lutjeharms et al. 1981), and from inertial recirculation in the southwest Indian Ocean (Harris 1972; Gründlingh 1980). The Agulhas Current flows southwestward along the eastern coast of southern Africa and separates from the coast near the southern tip of the continental slope at approximately 20°E. North of 35°S, the current tends to follow the continental slope closely. South of this latitude, the current develops lateral meanders whose amplitudes generally increase downstream (Lutjeharms 1981). After its separation from the African land mass, the Agulhas executes an abrupt anticyclonic (counterclockwise) loop and turns back into the Indian Ocean as an eastward flowing jet (Lutjeharms and van Ballegooyen 1984). The eastward flow is characterized by the presence of large-scale meanders that have been related to topographic features such as the Agulhas Plateau and the Mozambique Ridge extension (Harris 1970). The average volume transport of the Agulhas Current in the region south of South Africa has been estimated at 60 Sv ($1 \text{ Sv} \equiv 10^6 \text{ m}^3 \text{ s}^{-1}$) (Gründlingh

1980), although values as high as 130 Sv have been reported in its southern extension (Jacobs and Georgi 1977). While there is no conclusive evidence for the existence of any periodicity in the Agulhas transport (Gründlingh 1980), thermal infrared images and historical data indicate that the Agulhas Retroflexion penetrates farther to the west during the months of the austral summer (Lutjeharms and van Ballegooyen 1988a). Seasonal variability has also been reported in altimeter observations of certain limited areas of the Agulhas Retroflexion (Quartly and Srokosz 1993; Chelton et al. 1990; Feron et al. 1992).

The first attempt to model the dynamics of the Agulhas Current system was an analytical study presented by de Ruijter (1982). He showed that a linear, Munk-type model of the wind-driven circulation cannot reproduce a significant eastward turning of the Agulhas Current. Based upon largely qualitative arguments, de Ruijter suggested that inertia must be incorporated into any model that is to reproduce a significant retroflexion of the Agulhas Current.

Lutjeharms and van Ballegooyen (1984) used the free inertial model of Warren (1963) to study the path of the Agulhas Current. Their results show a farther westward penetration of the current for low than for high volume transports. In a later study Lutjeharms and van Ballegooyen (1988b) showed that on occasions the Agulhas Retroflexion occurs far upstream of its characteristic location. They attributed this bimodality of the retroflexion to changes in the volume transport and the effect of bottom topography on the current's path.

De Ruijter and Boudra (1985) carried out a series of numerical experiments using a nonlinear barotropic model with a flat bottom, forced by an analytical wind

Corresponding author address: Dr. Ricardo P. Matano, College of Oceanic and Atmospheric Sciences, Oregon State University, 104 Ocean Administration Building, Corvallis, Oregon 97331-5503.

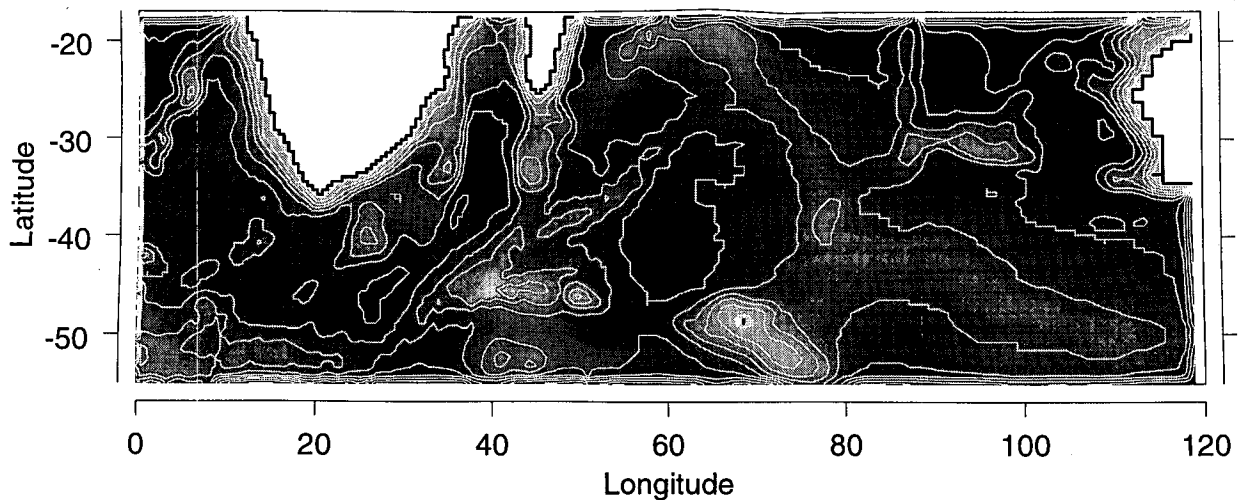


FIG. 1. Bottom topography of the southern Indian Ocean and the portion of the South Atlantic Ocean used with the model. Topographic data was obtained from the ETOPO5 dataset and smoothed using a five-point Laplacian smoother.

representation. In low Rossby number experiments, they observed that the entire transport of the modeled Agulhas Current flows westward around Africa into the South Atlantic Ocean. With increasing Rossby number, the anticyclonic circulation patterns in the subtropical Atlantic and Indian Oceans became isolated from each other. The authors suggested that the increase in the retroreflection strength with Rossby number was the result of a net accumulation of anticyclonic relative vorticity, generated as the current follows an inertially driven southward path after leaving the southern tip of the African continent.

Boudra and de Ruijter (1986) went a step beyond the earlier experiments by including vertical stratification in a three-layer model. They also observed that the strength of the retroreflection increased with Rossby

number. For the case with the greatest inertia the transfer of water from the Indian to the South Atlantic Ocean was mostly accomplished by the shedding of deep eddies that resulted from a downward transfer of surface momentum.

Ou and de Ruijter (1986) studied the effect of curvature of the coastline on the location where the Agulhas Current separates from the coast. Using a simple and elegant analytical model, they showed that a coastline with a curvature like the African coast reinforces the β effect in sharpening the anticyclonic shear of the current and induces a centrifugal force. Both effects tend to increase the cross-stream tilt of the thermocline, which leads to its surfacing at some equatorward latitude and the consequent separation of the current from the coast. The authors also showed that the separation is highly sensitive to the volume flux of the current. Increasing the transport forces a premature separation.

Boudra and Chassignet (1988) used an isopycnal model with a flat-bottomed ocean and a simplified coastline configuration to study the causes of the retroreflection. In a one-layer experiment the retroreflection was found to be the result of a balance between viscous and inertial forces and β advection. When density stratification was included by adding more layers, the stretching term in the vorticity balance became one of the most important mechanisms for the current retroreflection.

Chassignet and Boudra (1988) used the same numerical model to study the process of ring formation. The authors found that the frequency at which rings are formed depends on the shape of the African coastline, the degree of baroclinicity in the water column, and the inertia of the current. As the Rossby number and baroclinicity of the boundary current are increased (through thinning of the top layer), more fluid retroreflects into

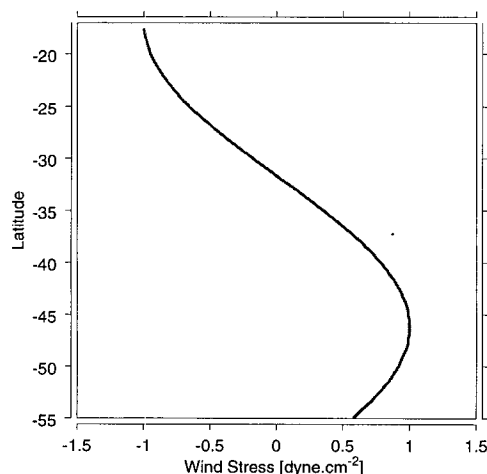


FIG. 2. Analytical wind stress distribution used to force the model.

TABLE 1. Numerical experiments.

Experiment	Resolution	Topography	Stratification	Wind forcing
1	0.5°	$H = 4000$ m	Barotropic	Analytical
2	0.5°	$H = 2000$ m	Barotropic	Analytical
3	0.5°	$H = 1000$ m	Barotropic	Analytical
4	0.5°	ETOPO5	Baroclinic	Analytical
5	1.0°	ETOPO5	Baroclinic	Analytical
6	0.5°	Heavily smoothed ETOPO5	Baroclinic	Analytical
7	0.5°	ETOPO5	Baroclinic	Climatological
8	0.5°	ETOPO5	Baroclinic	Analytical (zero wind stress curl moved 5° to the north)
9	0.5°	ETOPO5	Baroclinic	Analytical (zero wind stress curl moved 5° to the south)

the Indian Ocean and fewer rings are formed. With a 40-km grid resolution and a rectangular African coastline, the inertia and baroclinicity of the Agulhas Current must be relatively weak in order for rings to form. As the inertia increases, more fluid retroflects and fewer rings are formed.

Limited computational resources have restricted past numerical studies of the Agulhas Retroflection to cases with flat-bottomed basins and highly simplified geometry. For example, the experiments of de Ruijter and Boudra (1985), Boudra and de Ruijter (1986), Boudra and Chassignet (1988), and Chassignet and Boudra (1988) covered a basin that was only 1440 km long and 1280 km wide. The most realistic representation of coastal geometry in any of those studies was that of Boudra and Chassignet (1988), who used a quadrilateral shape to simulate the African coastline. Although much insight into Agulhas dynamics has been obtained by these pioneering studies, it seems reasonable to ask whether the inclusion of more realistic features, including coastal geometry, bottom topography, and climatological winds, may alter the conclusions of these previous studies. This article describes the results of replicating some previous numerical experiments in this more realistic setting. The conclusion of these experiments is that the inclusion of coastal geometry and bottom topography of the Indian Ocean produces qualitative differences from past results. In particular, it will be shown that the retroflection of the Agulhas Current

appears to be more closely related to the effect of bottom topography than to the inertial effects suggested previously.

This article has been organized as follows: after this introduction, section 2 provides a brief description of the numerical model used in these experiments and a discussion of the model setup. Section 3 contains a description of the experiments. In section 4 is a summary and discussion of the results.

2. Model description

The numerical model used in this study is the Princeton Ocean Model. This model solves the primitive equations in vertical sigma coordinates for the three-dimensional fields of velocity, temperature, salinity, turbulent energy, and length scale. Horizontal diffusion in the model is handled by a term of Laplacian form ($A_M = 2000 \text{ m}^2 \text{ s}^{-1}$), while vertical mixing is parameterized with the second-order turbulence closure scheme of Mellor and Yamada (1982). A more detailed description of the model and its numerical algorithms can be found in Blumberg and Mellor (1987).

Figure 1 shows the bottom topography of the basin used in the numerical experiments. The bottom depths shown in Fig. 1 were obtained from the ETOPO5 dataset. To reduce errors associated with the pressure gradient in sigma coordinates, the original bottom depths were smoothed using a five-point Laplacian smoother and bottom slopes were adjusted so that the maximum value of the parameter $\delta D/D < 0.3$, where D is the ocean depth and δD is the depth difference between adjacent grid points (Haney 1991; Mellor et al. 1994). The model has 15 vertical levels and a horizontal resolution of approximately one-half degree in latitude and longitude.

The lateral boundaries of the model are all closed. To prevent spurious reflections we have implemented a region of increased viscosity along the western boundary of the model. To confirm that this is an adequate precaution, we have replicated our more important simulation in a domain that encompasses all the South Atlantic and south Indian basins using a 1°

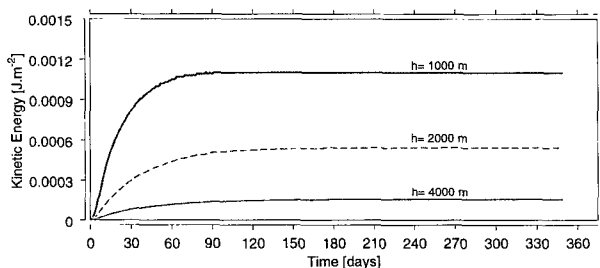


FIG. 3. Time evolution of the basin-averaged kinetic energy in experiments 1–3.

model. These experiments will be discussed in detail in the next section.

Two types of wind stress forcing were used in the numerical experiments: an analytical expression that

simulates the annual, zonally averaged wind stress over the south Indian Ocean and the climatological wind stress values compiled by Hellerman and Rosenstein (1983). The use of an analytical expression for the

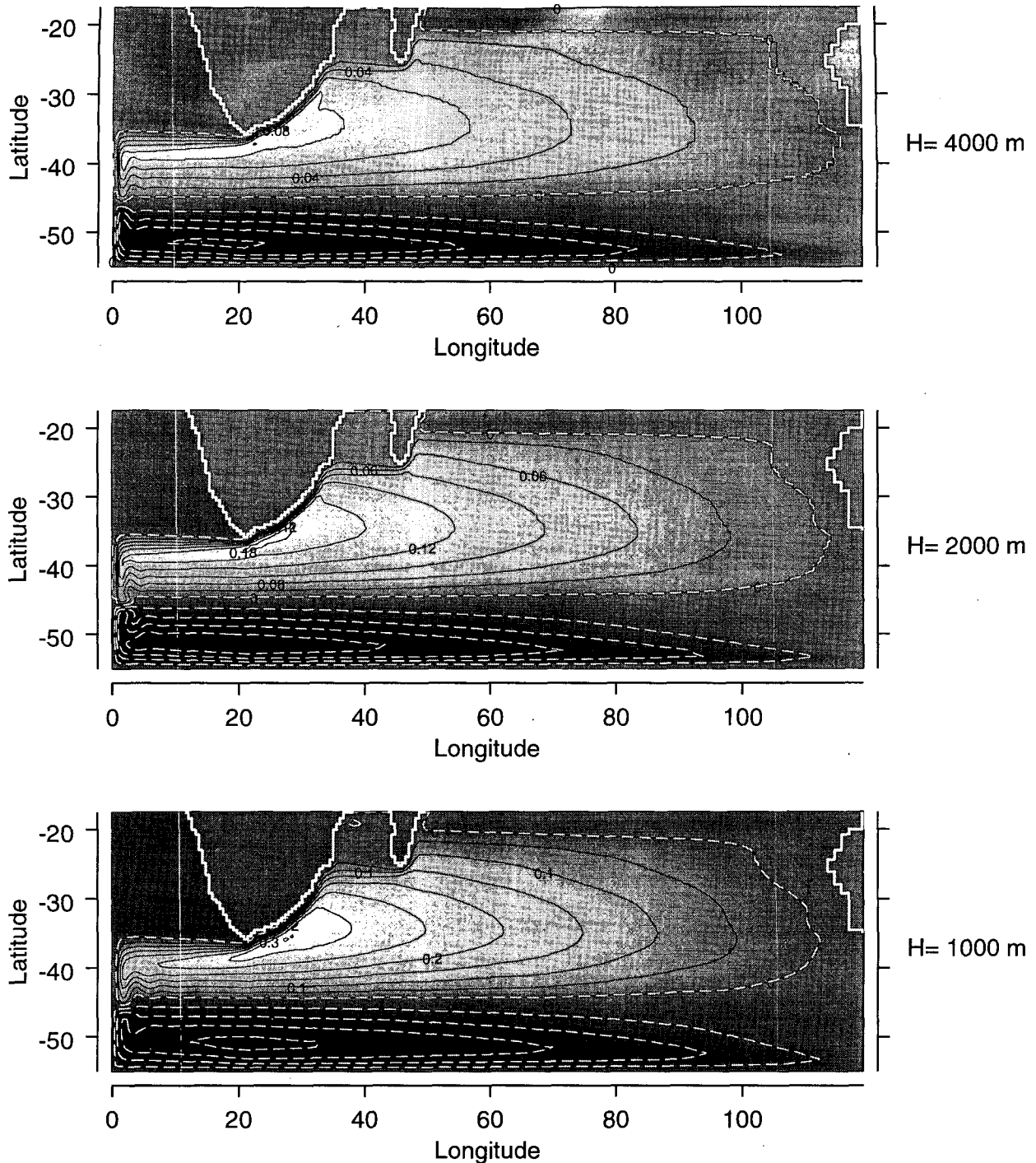


FIG. 4. Sea surface elevation distributions corresponding to the flat-bottomed, barotropic experiments (experiments 1-3) for basin depth (a) 4000 m, (b) 2000 m, (c) 1000 m.

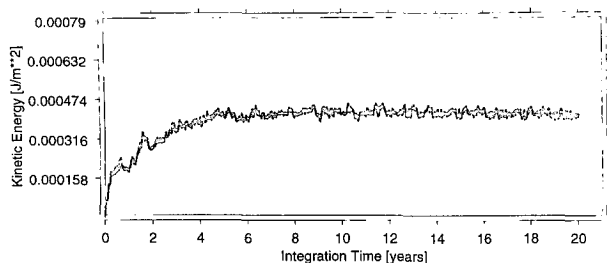


FIG. 5. Time evolution of the basin-averaged kinetic energy of a basin with a realistic representation of bottom topography (experiment 4).

wind stress forcing facilitates the study of the effects on the oceanic circulation of changing wind patterns. Use of climatological wind stress values allows a direct comparison between model results and observations. Figure 2 shows the zonal component of the analytical wind stress forcing. It has a zero value in the South Atlantic sector and increases smoothly with longitude to the south Indian Ocean. The zero of the wind stress curl is located at 45°S in agreement with climatological observations (Hellerman and Rosenstein 1983).

3. Numerical experiments

In this section we will describe the series of numerical experiments used to investigate the causes of the Agulhas Retroflexion. Table 1 summarizes the distinctive characteristics of each experiment and indicates the sequence in which they will be described. The first three cases correspond to a flat-bottomed basin with the dimensions and coastline geometry shown in Fig. 1. The aim of these experiments is to demonstrate that, in a flat-bottomed, realistically shaped Indian basin, most of the transport of the Agulhas Current flows into the South Atlantic Ocean for realistic values of the global Rossby number. Experiment 4 includes the ETOPO5 bottom topography and illustrates the effect of topographic torque on the Agulhas Retroflexion. This experiment will be the benchmark for comparison with the later experiments. The remaining five experiments investigate the sensitivity of the Agulhas Retroflexion to changes in wind forcing, density stratification, basin dimensions, and topographic smoothing.

a. The Agulhas Retroflexion in a flat-bottomed Indian basin

This section discusses the results of the first three experiments listed in Table 1. The purpose of these experiments is to show that in the present model inertia does not appear to play a significant role in forcing the Agulhas Retroflexion. It is argued that the discrepancy between these results and previous simulations might be related to coastline geometry.

In the numerical experiments of de Ruijter and Boudra (1985) and Boudra and de Ruijter (1986) the African continent was represented by a rigid meridional boundary in the middle of a rectangular basin. Boudra and de Ruijter (1986) pointed out that this particular shape maximizes the importance of the β effect and therefore artificially increases the strength of the retroflexion. The effects of a northeast trend of the bounding coast on the Agulhas Retroflexion was investigated by Boudra and Chassignet (1988) and Chassignet and Boudra (1988) who, using a three-layer model, concluded that a coastline with this form could significantly weaken the retroflexion. To quantify this effect we have conducted experiments in a flat-bottomed basin with the dimensions and coastline geometry of the Indian Ocean. In these experiments, the inertia of the flow is controlled by the basin depth, with deeper basins corresponding to the less inertial cases (de Ruijter and Boudra 1986). Although we have conducted experiments in barotropic and baroclinic modes for consistency with past studies, we will show only the steady states of barotropic runs; the baroclinic experiments do not significantly differ from the barotropic ones. All experiments were started from a state of rest and run until a dynamical equilibrium between the ocean circulation and the wind stress forcing was achieved. Figure 3 shows the time adjustment of the model, as measured by the temporal evolution of the basin-averaged kinetic energy, for the three basin depths indicated in Table 1. Since these particular experiments did not include density effects, the model adjustment is mostly accomplished by the propagation of long barotropic planetary waves. These waves have relatively high phase speeds, so the model typically reaches equilibrium after approximately one month. Figure 4 shows the steady-state distribution of sea surface elevation in the three flat-bottomed experiments. For large-scale quasigeostrophic circulation, sea surface elevation can be taken as a proxy of the streamfunction of the flow. The upper panel of Fig. 4 shows the sea surface elevation in a basin 4000 m deep. There is an anticyclonic gyre in the Indian Ocean and along the eastern coast of the African continent a southward-flowing western boundary current. In this case there is no significant Agulhas Retroflexion. After reaching the tip of the continent the western boundary current flows directly into the South Atlantic Ocean. Retroflexion is induced if the basin depth is decreased (middle and lower panels of Fig. 4). In these cases the increased inertia of the flow forces the Agulhas Current to enter the open ocean as a free inertial jet. In this free jet, changes in the Coriolis parameter are compensated by opposite changes in the relative vorticity of the current, which eventually forces retroflexion. It is apparent from Fig. 4, however, that even the most inertial of the cases presented (experiment 3) has a relatively weak Agulhas Retroflexion, with more than 90% of the Agulhas transport flowing from the Indian into the South Atlan-

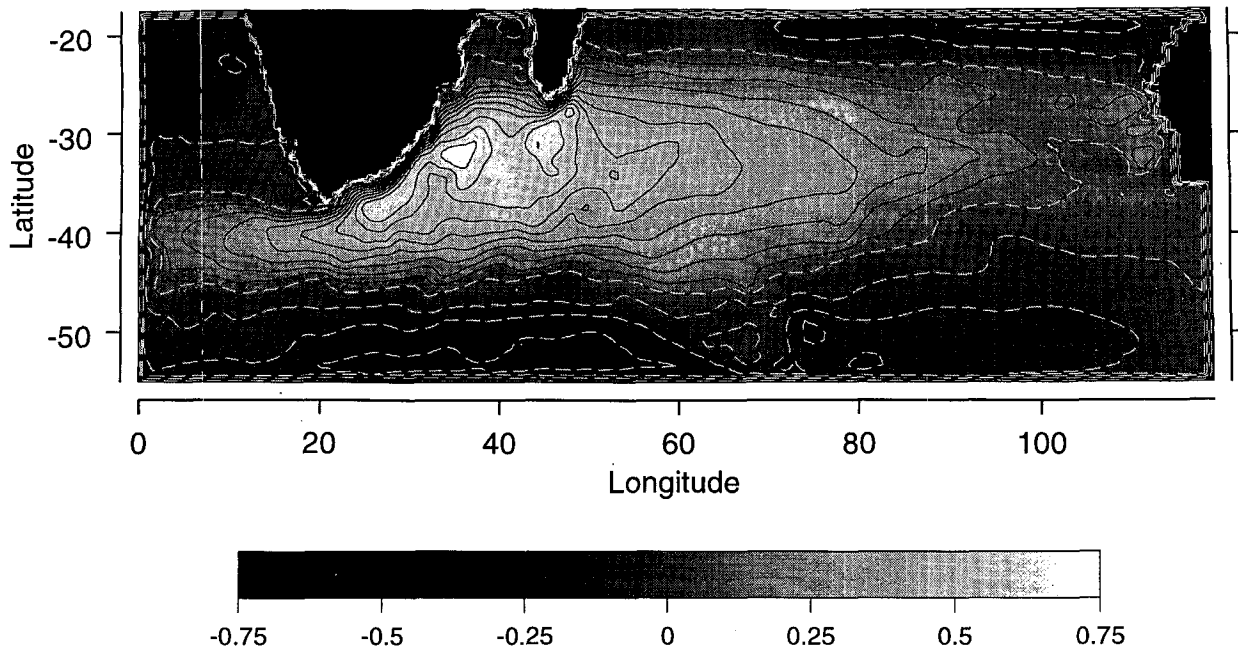


FIG. 6. Steady-state distribution of the sea surface elevation in experiment 4, which included a realistic representation of the bottom topography.

tic Ocean. The differences in retroreflection strength between these experiments and those reported previously (de Ruijter and Boudra 1985; Boudra and de Ruijter 1986; Boudra and Chassignet 1988; Chassignet and Boudra 1988) can be rationalized in terms of coastline azimuth. At difference with previous experiments where the African continent is represented by a meridional wall, the African coastline has an azimuth of approximately 40° . This coastline trend induces a westward component of the inertial forces that weakens the retroreflection as observed. It is, of course, possible to get a robust retroreflection by a further decrease of the basin depth, but then the inertial effects stiffen the circulation to a highly unrealistic degree.

Boudra and Chassignet showed that, if in an isopycnal model the depth of the upper layer is decreased to a value of 300 m, approximately 50% of the total transport (mostly in the upper layer) would retroreflect. In contrast to an isopycnal model, in a level model it is more difficult to control the inertia of the upper flow. In the next section instead, we will show that a significant retroreflection can be obtained by including the bottom topography of the Indian basin.

b. Experiments with realistic bottom topography

Experiment 4 includes a realistic representation of the bottom topography of the southern Indian Ocean (Fig. 1). The model was initialized with an analytical density profile that approximates the spatially averaged density profile of the southern Indian Ocean. There are

two reasons why this averaged profile is used in our sensitivity experiments rather than the climatological density values: First, it is desirable to control the density field so that the stratification of the Indian Ocean may be changed to observe how these changes affect the retroreflection of the Agulhas Current. Second, the climatological density values depend upon the true location of the retroreflection, and this will complicate the physical interpretation of our process-oriented experiments.

The model is started from a state of rest and run until dynamical equilibrium. In numerical models initialized with climatological density values (e.g., Matano and Philander 1993; Ezer and Mellor 1994), the dynamic adjustment between the ocean circulation and the wind stress forcing is mostly associated with advective processes and is relatively fast. Typically, these integrations reach a quasistationary state in a couple of months. This is because the thermocline of those models already have an east–west slope that geostrophically compensates the wind stress forcing. By contrast, in the present experiments the thermocline is initially flat, and the ocean adjustment is not so much related to advective process as to the slow propagation of baroclinic planetary waves and the buildup of a longitudinal thermocline tilt. The model's adjustment, as indicated by the time evolution of the basin-averaged kinetic energy (Fig. 5), occurs in three periods. First there is a rapid rise in kinetic energy, occurring over a few months time, related to the propagation of barotropic modes. Following the barotropic adjustment there is a

slower rise in kinetic energy, between 2 months and 4 years, associated with the propagation of baroclinic modes. After the fifth year of integration the model reaches dynamical equilibrium with the wind forcing. The numerical experiments to be discussed in this article were run for a period of 20 years.

The steady-state sea surface elevation is shown in Fig. 6. The inclusion of bottom topography has generated a realistic retroflexion of the Agulhas Current, even though the average depth of the basin is more than 3000 m. The topographically forced retroflexion returns approximately 80% of the Agulhas transport to the southern Indian Ocean. Bottom topography also induces a secondary retroflexion of the East Madagascar Current. This retroflexion is related to the presence of the Madagascar Ridge, and its existence has been documented by in situ and remote observations (Lutjeharms et al. 1981). The mass transport of the Agulhas Current has a maximum of 62 Sv close to the African continent, a value close to that indicated by the Sverdrup balance but smaller than the values of approximately 100 Sv reported based upon hydrographic calculations (Gründlingh 1980; Bennett 1988; Lutjeharms and van Ballegooyen 1988a). This discrepancy may be due to the fact that this is not an eddy resolving model so that the intense recirculation that is thought to occur in the southern portion of the Agulhas Current is not captured.

A vorticity analysis of the steady-state circulation allows quantitative statements about the effect of the bottom topography. The vertically integrated vorticity equation can be obtained by taking the curl of the momentum equations for the vertically averaged velocity components (e.g., Ezer and Mellor 1994). The resulting equation can then be written as

$$\begin{aligned} \frac{\partial}{\partial t} \left[\frac{\partial \bar{v}D}{\partial x} - \frac{\partial \bar{u}D}{\partial y} \right] + \frac{\partial A_y}{\partial x} - \frac{\partial A_x}{\partial y} + \frac{\partial (f\bar{u}D)}{\partial x} \\ + \frac{\partial (f\bar{v}D)}{\partial y} = \frac{\partial P_b}{\partial x} \frac{\partial D}{\partial y} - \frac{\partial P_b}{\partial y} \frac{\partial D}{\partial x} \\ + \frac{\partial (\tau_{y0} - \tau_{yb})}{\partial x} - \frac{\partial (\tau_{x0} - \tau_{xb})}{\partial y}, \quad (1) \end{aligned}$$

where \bar{u} and \bar{v} are the vertically averaged velocity components, A_x and A_y are the horizontal advection and diffusion terms, f is the Coriolis parameter, τ_{x0} and τ_{y0} are the surface stress terms, τ_{xb} and τ_{yb} are the bottom stress terms, and P_b is the bottom pressure term. For steady-state flow, the first term of (1) vanishes and, since

$$\frac{\partial (\bar{u}D)}{\partial x} + \frac{\partial (\bar{v}D)}{\partial y} = 0,$$

the term that contains the Coriolis parameter reduces to $\beta \bar{v}D$, where $\beta = df/dy$. The different terms of (1)

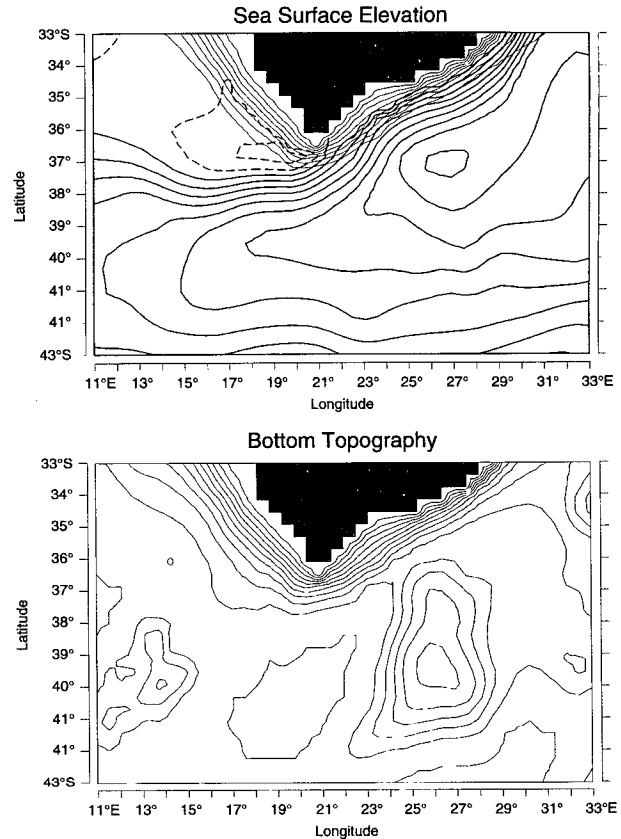


FIG. 7. Expanded view of the sea surface elevation and bottom topography of the Agulhas retroflexion.

have been calculated from the model results and the results are displayed in Figs. 8 and 9.

As a reference for the discussion of the vorticity balances, Fig. 7 displays an expanded view of the sea surface elevation and bottom topography of the Agulhas Retroflexion. Figure 8 shows a zonal section of the vorticity balance at 39°S, the approximate axis of the retroflexion. Figure 8 indicates that from a dynamical point of view there are actually two retroflexions. The first, centered at approximately 26°E, is associated with the shallow region of the Agulhas Plateau. The second retroflexion occurs near 14°E and is related to the blocking effect of the Agulhas Ridge. Near the Agulhas Plateau, the main balance is between bottom pressure torque and the β term. In this area the flow closely follows the f/D contours. To the west of the peak of the Agulhas Plateau, at approximately 26°E, the current flows south and the β torque is positive, that is, anti-clockwise. To accommodate the changes in planetary vorticity, the current flows into deeper waters. To the east of the Agulhas Plateau the flow is northward (see Fig. 7) to a region where the Coriolis parameter is smaller, so that the associated torque changes sign. In the region close to the Agulhas Ridge the balance is

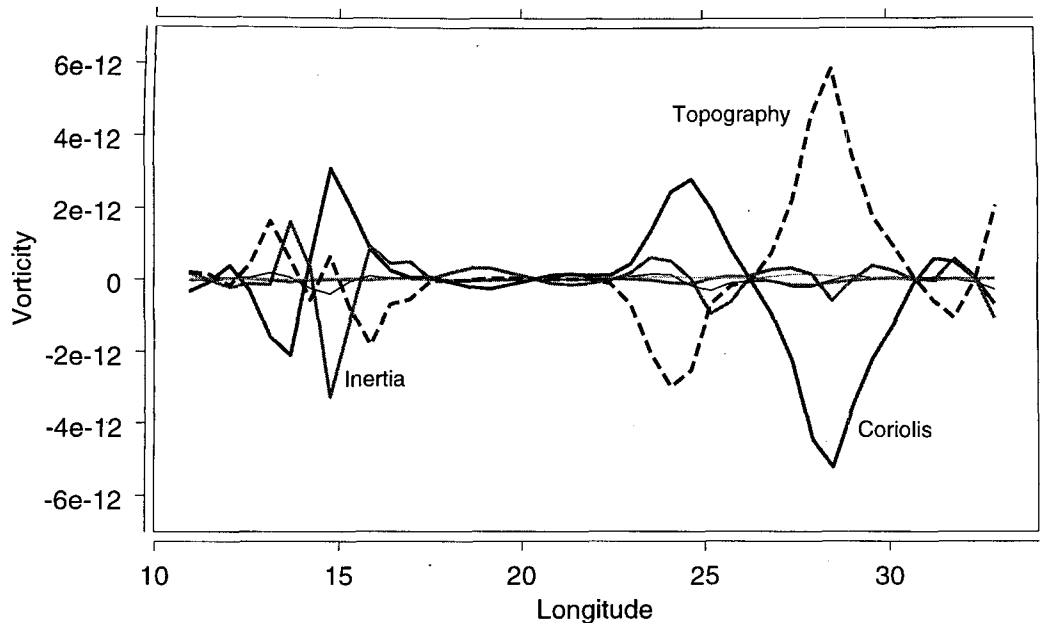


FIG. 8. Vorticity balance along 39°S and between 11° and 33°E.

similar to that over the Agulhas Plateau with stronger inertial effects that cause a portion of the Agulhas Current to flow into the South Atlantic Ocean, crossing the potential vorticity contours associated with the Agulhas Ridge. The lack of prominent features between the Agulhas Plateau and the Agulhas Ridge, in the vorticity balance shown in Fig. 8, reflects the quasi-zonality of the flow.

Figure 9 shows the regional distribution of the two most important terms of (1) the β and bottom torques. Over the Agulhas Plateau the dominant balance is between the bottom pressure torque and the β term. A similar balance is apparent over the Agulhas Ridge, although in this area there is also a contribution from the inertial torque, which forces a portion of Agulhas Current to cross the f/D contours and flow into the South Atlantic Ocean (Fig. 8). In this region of the ocean, where the flow has a strong zonal component, inertial effects tend to weaken the Agulhas Retroflexion. As predicted by the numerical experiments of de Ruijter, Boudra, and Chassignet, inertial effects force the Agulhas Current to leave the continental slope of the African continent and to turn offshore at approximately 37°S. Once the current leaves the coast, the inertial effects become weaker and the current path is more strongly influenced by the underlying bottom topography.

The branching and double retroflexion of the Agulhas Current observed in our numerical experiments is supported by in situ and remote observations. Bennett (1988) reported that during a 1985 hydrographic cruise the Agulhas Current retroflected in two branches. The first, located near 20°E, contained the current warm

core ($T > 24^{\circ}\text{C}$) and carried about one-third of its total transport. The second branch, located in the neighborhood of 15°E, contained the remaining two thirds of the incoming transport plus an important contribution from local recirculation. Lutjeharms (1988a,b), studying infrared images, observed that although the main surface signal of the Agulhas occurs in the neighborhood of 20°E, a retroflecting branch can also be observed as far west as 8°E. Strong support to the hypothesis of topographic control of the Agulhas flow was also given by Lutjeharms and van Ballegooyen (1988b), who noted that a significant portion of the Agulhas transport diverts just south of Port Elizabeth. They noted that this location corresponds to a topographic gap between the continental shelf and the Agulhas Plateau. Gordon et al. (1987) discussed the Agulhas kinematics from hydrographic observations collected in late 1983. They noted that, although a large portion of the flow retroflects at around 21°E, the western limit of the retroflexion falls close to 14°E.

c. Model sensitivity

The results of the previous section indicate that, in this model, bottom topography can induce a realistic retroflexion of the Agulhas Current. In this section we investigate the sensitivity of those results to changes in basin size, topographic smoothing, wind stress distribution, and vertical stratification. The aim of these experiments is to test the robustness of the numerical experiments and to illustrate the qualitative changes that should be expected from changes in the model configuration.

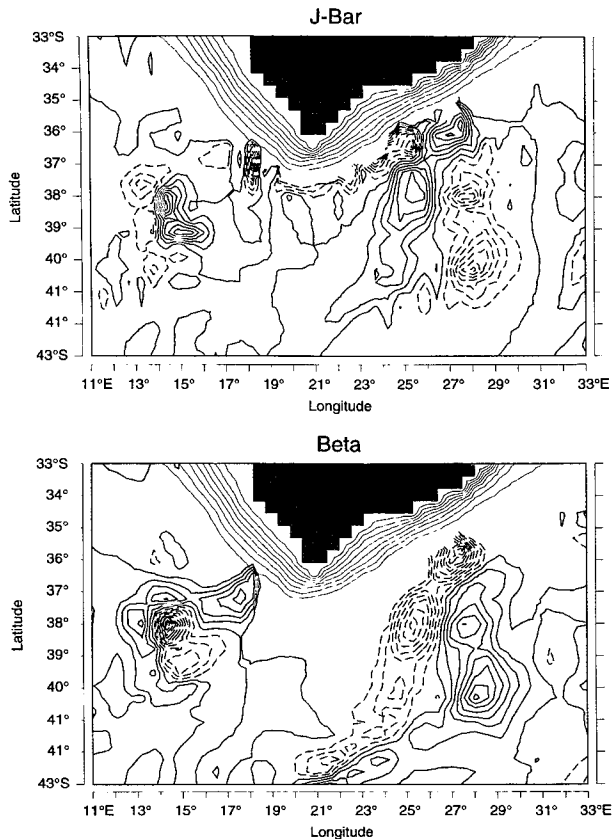


FIG. 9. Regional distribution of the two most important components of the vorticity balance in the Agulhas retroreflection: the topographic torque (upper panel) and the Coriolis torque (lower panel). Notice the close correspondence between these two terms over the Agulhas Plateau and the Agulhas Ridge.

An early concern when designing this numerical study was the possible effect of the western boundary of the model basin on the modeled Agulhas dynamics. This artificial boundary was placed away from the location where the real Agulhas Current is observed to retroreflect in order to minimize any impact on the retroreflection dynamics. A region of increased viscosity was added near the western boundary to prevent spurious reflections. Since these precautions may be insufficient to ensure that the modeled Agulhas Retroreflection is not affected by the location of the western wall, we have repeated some of the more important simulations in a domain that encompasses all of the South Atlantic and south Indian basins with a model with one-degree resolution. As an example of these simulations, Fig. 10 shows the steady-state sea surface elevation for experiment 5, with all other model parameters as in the benchmark case (experiment 4), but with the expanded domain and decreased resolution. Figure 10 shows a robust retroreflection of the Agulhas Current at the southern tip of the African continent, indicating that the results of

the regional model (experiment 4) are not affected by the location of the western boundary.

Experiment 6 demonstrates the effects of topographic changes on the location and strength of the retroreflection. Figure 11 shows the steady-state sea surface elevation for this, in which the original bottom topography was heavily smoothed. The resulting circulation pattern shows a sensible weakening of the retroreflection, particularly over the Agulhas Plateau. In this experiment, between 60% and 70% of the incoming Agulhas transport flows into the South Atlantic, in contrast to the 20%–30% of the benchmark experiment (experiment 4). Experiment 6 illustrates the important role that proper resolution of bottom topography might play in the modeling of the Agulhas Current. This has also been noted by Lutjeharms and Webb (1995) who in a comparison between climatological observations and the numerical results of the Fine Resolution Antarctic Model (FRAM) pointed out that in that model the Agulhas Retroreflection occurs farther upstream than its observed location. Lutjeharms and Webb (1995) attributed this discrepancy to a poor model resolution of the bottom topography in the region close to the Agulhas Plateau.

To study the sensitivity of the Agulhas Retroreflection to changes in the wind stress forcing we have conducted three additional experiments (experiments 7–9). In experiment 7 the analytical wind stress was replaced by the climatological annual mean values from Hellerman and Rosenstein (1983). Experiments 8 and 9 demonstrate the effect that changes in the wind stress curl has on the location and strength of the Agulhas Retroreflection. Figure 12a shows the steady-state distribution of the sea surface elevation for experiment 7. It is apparent from a comparison of Fig. 12a with Fig. 6 (experiment 4) that the introduction of climatological winds have no major qualitative effect on the location of the Agulhas Retroreflection, or its strength. The most obvious difference between Fig. 6 and Fig. 12a is the east–west tilt of the subtropical convergence zone in Fig. 12a. This tilt is related to longitudinal variations in the climatological winds that were absent in the analytical case. Figures 12b and 12c shows the results of numerical experiments in which the zero of the wind stress curl was displaced 5° to the North and South from its mean position at 45°S (experiments 8 and 9, respectively). de Ruijter and Boudra (1986) have already investigated this problem using a nonlinear, barotropic model in a flat-bottomed basin. They concluded that the distance between the latitude of zero wind stress curl and the southern tip of the African peninsula is one of the primary factors that determine the degree of isolation of the anticyclonic gyres east and west of the African continent. The results displayed in Fig. 12b, however, indicate that although a northward shift of the gyre tends to isolate the south Indian circulation from the Atlantic gyre, an equivalent southward displacement (Fig. 12c) does not greatly increase the amount

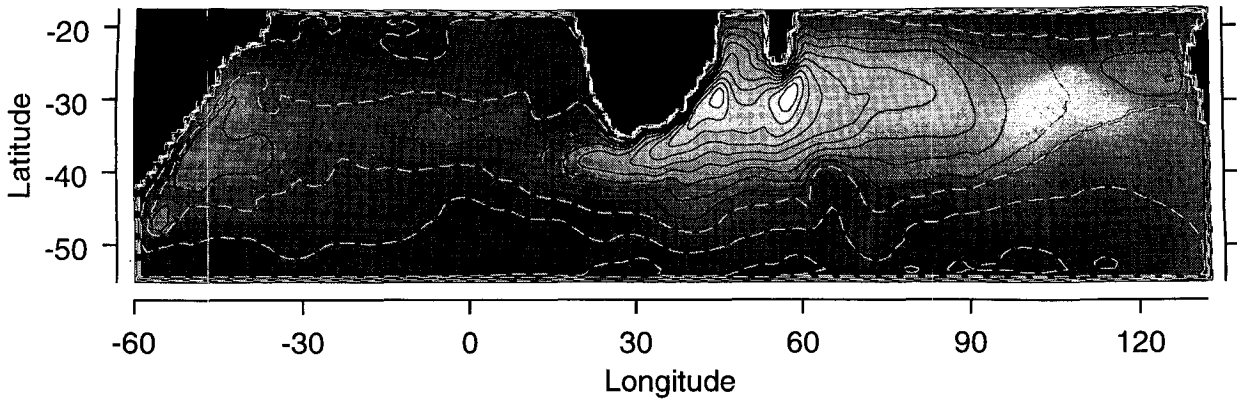


FIG. 10. Steady-state distribution of the sea surface elevation in experiment 5. In this experiment the model domain was extended to investigate the possible effects of the artificial western boundary in previous experiments.

of Agulhas water flowing into the South Atlantic. In fact, in experiment 9 the increase in the amount of Agulhas water that is spilled over into the South Atlantic is less than 10% more than in the benchmark case (experiment 4), due to the locking effect of the bottom topography. Notice in Fig. 12c that although the Agulhas Return Current follows the poleward displacement of the zero of the wind stress curl, the axis of the retroreflection remains as in experiment 4 (Fig. 6).

A final series of experiments investigated the sensitivity of the Agulhas Retroreflection to changes in density stratification. The results (not shown) indicate that, at least in our non-eddy-resolving experiments, the retroreflection does not appear to be very sensitive to moderate density changes. It is interesting to note that a strong decrease, or increase, in baroclinicity tends to

weaken the retroreflection. In the first case the weakening is related to a decoupling of the upper and bottom circulation, while in the later case it is attributed to a general decrease of the Agulhas transport caused by the existence of meridional ridges that inhibit the westward propagation of wind energy from the eastern Indian Ocean to the African coast. Our experiments indicate that in the limit of a complete barotropic system the Agulhas Current ceases to exist and the Madagascar Current takes the role of the western boundary current of the southern Indian Ocean.

4. Summary and discussion

The goal of this study was to investigate the causes of the Agulhas Retroreflection using a 3D primitive equa-

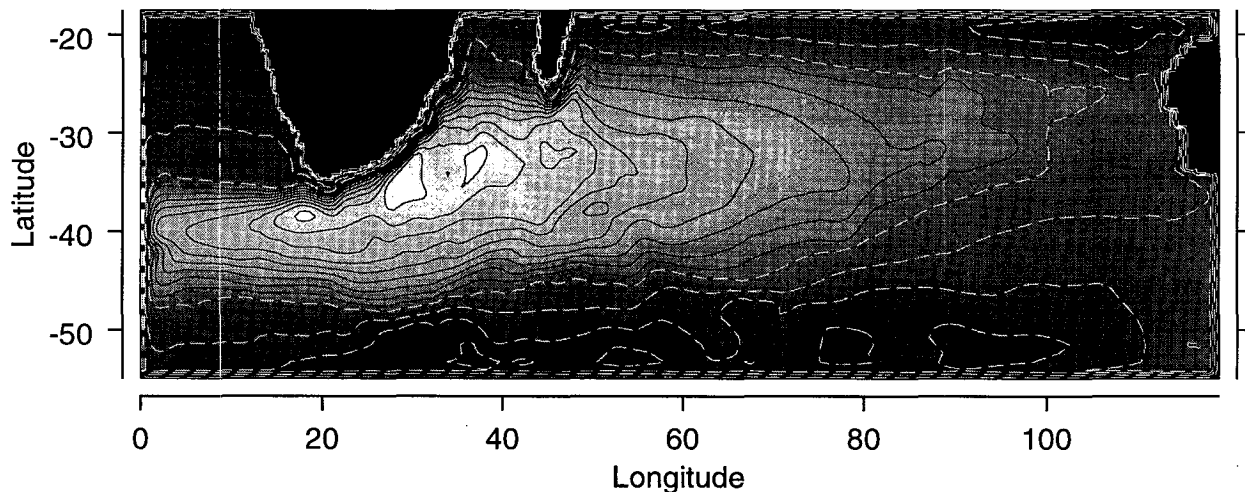


FIG. 11. Steady-state distribution of the sea surface elevation in experiment 6. In this experiment the bottom topography was heavily smoothed. Notice that, as the topographic control weakens, the amount of Agulhas water that flows into the South Atlantic is increased.

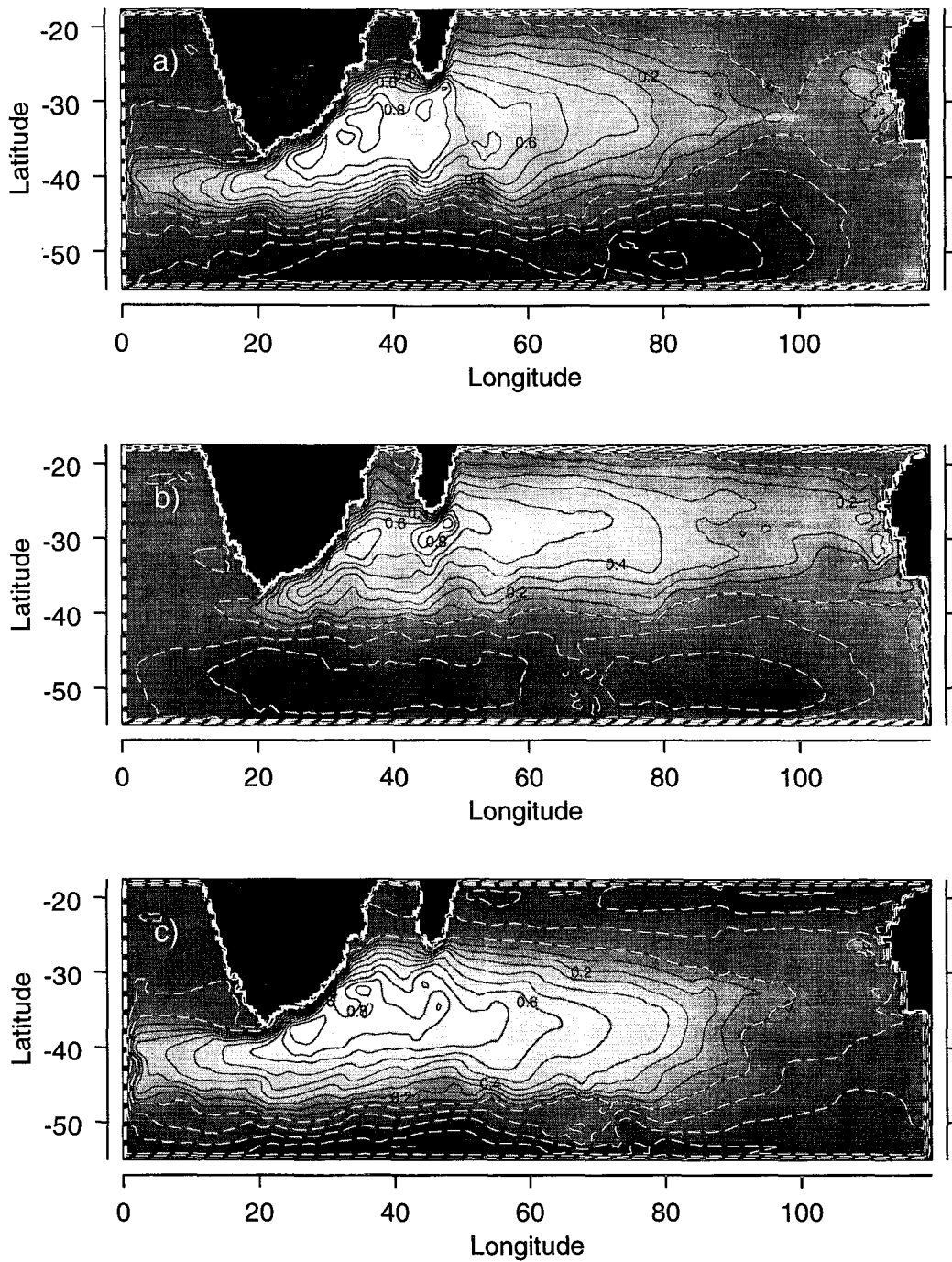


FIG. 12. Steady-state distribution of the sea surface elevation in experiments 7–9. In these experiments the wind forcing used previously was replaced by (a) climatological wind stress data (Hellerman and Rosenstein 1983), (b) an analytical distribution similar to that shown in Fig. 2 but with the zero of the wind stress curl moved 5° to the north, and (c) as in (b) but the zero of the wind stress curl moved 5° to the south.

tion model. The general characteristics of these experiments are listed in Table 1. Experiments 1 to 3, conducted in a basin with realistically shaped coastlines but a flat bottom, were characterized by a weak retro-

flexion, with more than 90% of the Agulhas transport flowing into the South Atlantic basin. When a realistic representation of the bottom topography was incorporated in the model (experiment 4), the amount of water

transferred to the South Atlantic was reduced to 20%–30% of the total Agulhas transport. A vorticity balance of the steady-state solution indicates the existence of two retroreflections. The first is associated with the Agulhas Plateau at the southern tip of the African continent, and the second with the Agulhas Ridge between 10° and 15°E. These two retroreflecting branches have already been documented in observational studies of this region (Bennett 1988; Gordon et al. 1987; Lutjeharms 1988a,b). Experiments to test the sensitivity of these results to changes in basin size, topographic smoothing, wind stress forcing, and density stratification were carried out. For the range of values of the parameters tested, these experiments confirmed that bottom topography has a major effect on the position and strength of the Agulhas Retroreflection. An experiment with highly smoothed bottom topography (experiment 5) demonstrated the importance of model resolution in the simulation of the Agulhas Retroreflection. The series of experiments using different wind forcing (experiments 7–9) indicate that the location of the simulated Agulhas Retroreflection might be more sensitive to equatorward than poleward displacements of the wind stress curl.

The model results discussed in this manuscript lack one of the more notable features of the Agulhas Retroreflection, namely, the intermittent formation and detachment of warm eddies (Olson and Evans 1986). A legitimate concern is whether a non-eddy-resolving model can capture the time-mean circulation of an eddy-populated region. In this regard it is important to differentiate cause and effects. The assumption underlying the present study is that the Agulhas Retroreflection is cause and the eddy effects. Eddies might interact, as they do, with the mean flow inducing time variability in the retroreflection, but these interactions can still be regarded as perturbations to a mean state that, to zero order, is determined by external factors. Similar examples are the separation of the Gulf Stream or the Brazil Current from the coast. Although both phenomena also occur in eddy-populated regions, neither of them is thought to be driven by eddies. In the particular case of the Agulhas Retroreflection, hydrographic observations (e.g., Lutjeharms and van Balegooyen 1984; Gordon et al. 1987; Bennett 1988) consistently indicate that the abrupt reversal of the flow occurs either near the Agulhas Plateau or the Agulhas Ridge—the two locations predicted by the model. Lutjeharms and Webb's (1993) analysis of FRAM results also showed a strong topographic steering of the simulated retroreflection, which, in spite of a continuous eddy shedding, remained locked to the Agulhas Plateau. To further address this issue we have studies in progress using an eddy-resolving version of the present model that investigates the role of bottom topography on the formation of those eddies and the dependence of the Agulhas Retroreflection on factors such as volume transport and local wind forcing.

Acknowledgments. This article benefited from the comments of M. G. Schlax and two anonymous reviewers. This research was supported by NSF Grant OCE-9402856.

REFERENCES

- Bennett, S. L., 1988: Where three oceans meet: The Agulhas retroreflection region. Ph.D. thesis, Massachusetts Institute of Technology/Woods Hole Oceanographic Institute, WHOI-88-51, 217 pp.
- Blumberg, A. F., and G. L. Mellor, 1987: A description of a three-dimensional coastal ocean circulation model. *Three-Dimensional Coastal Ocean Models*, N. Heaps, Ed., Coastal Estuarine Science, Vol. 4, Amer. Geophys. Union, 1–16.
- Boudra, D. B., and W. P. M. de Ruijter, 1986: The wind-driven circulation of the South Atlantic–Indian Ocean. II. Experiments using a multi-layer numerical model. *Deep-Sea Res.*, **33**, 447–482.
- , and E. P. Chassignet, 1988: Dynamics of the Agulhas retroreflection and ring formation in a numerical model. Part I: The vorticity balance. *J. Phys. Oceanogr.*, **18**, 280–303.
- Chassignet, E. P., and D. B. Boudra, 1988: Dynamics of Agulhas retroreflection and ring formation in a numerical model. Part II: Energetics and ring formation. *J. Phys. Oceanogr.*, **18**, 304–319.
- Chelton, D. B., M. G. Schlax, D. L. Witter, and J. G. Richman, 1990: Geosat altimeter observation of the surface circulation of the Southern Ocean. *J. Geophys. Res.*, **95**, 17 877–17 903.
- de Ruijter, W. P. M., 1982: Asymptotic analysis of the Agulhas and Brazil current systems. *J. Phys. Oceanogr.*, **12**, 361–373.
- , and D. B. Boudra, 1985: The wind-driven circulation in the South Atlantic–Indian Ocean. I. Numerical experiments in a one-layer model. *Deep-Sea Res.*, **32**, 557–574.
- Ezer, T., and G. L. Mellor, 1994: Diagnostic and prognostic calculations of the North Atlantic circulation and sea level using a sigma coordinate ocean model. *J. Geophys. Res.*, **99**, 14 159–14 171.
- Feron, R. C. V., W. P. M. de Ruijter, and D. Oskam, 1992: Ring shedding in the Agulhas Current system. *J. Geophys. Res.*, **97**, 9467–9477.
- Gordon, A. L., J. R. E. Lutjeharms, and M. L. Gründlingh, 1987: Stratification and circulation at the Agulhas retroreflection. *Deep-Sea Res.*, **34**, 565–599.
- Gründlingh, M. L., 1980: On the volume transport of the Agulhas Current. *Deep-Sea Res.*, **27A**, 557–563.
- Haney, R. L., 1991: On the pressure gradient force over steep topography in sigma coordinate ocean models. *J. Phys. Oceanogr.*, **21**, 610–619.
- Harris, T. F. W., 1970: Planetary-type waves in the South West Indian Ocean. *Nature*, **227**, 1043–1044.
- , 1972: Sources of the Agulhas current in the spring of 1964. *Deep-Sea Res.*, **19**, 633–650.
- Hellerman, S., and M. Rosenstein, 1983: Normal monthly wind stress over the world ocean with error estimates. *J. Phys. Oceanogr.*, **13**, 1093–1104.
- Jacobs, S. S., and D. T. Georgi, 1977: Observations on the southwest Indian/Antarctic Ocean. *A Voyage of Discovery*, M. Angel, Ed., Pergamon Press, 43–84.
- Lutjeharms, J. R. E., 1981: Spatial scales and intensities of circulation in the ocean areas adjacent to South Africa. *Deep-Sea Res.*, **28**, 1289–1302.
- , and R. C. van Ballegooyen, 1984: Topographic control in the Agulhas current system. *Deep-Sea Res.*, **31**, 1321–1337.
- , and —, 1988a: The retroreflection of the Agulhas Current. *J. Phys. Oceanogr.*, **18**, 1570–1583.

- , and ———, 1988b: Anomalous upstream retroflexion in the Agulhas Current. *Science*, **240**, 1770–1772.
- , and D. J. Webb, 1995: Modeling the Agulhas Current system with FRAM (Fine Resolution Antarctic Model). *Deep-Sea Res.*, **42**, 523–551.
- , N. D. Bang, and C. P. Duncan, 1981: Characteristics of the currents east and south of Madagascar. *Deep-Sea Res.*, **28A**, 879–899.
- Matano, R. P., and S. G. H. Philander, 1993: Heat and mass balances of the South Atlantic Ocean calculated from a numerical model. *J. Geophys. Res.*, **98**, 977–984.
- Mellor, G. L., and T. Yamada, 1982: Development of a turbulence closure model for geophysical fluid problems. *Rev. Geophys.*, **20**, 851–875.
- , T. Ezer, and L.-Y. Oey, 1994: The pressure gradient conundrum of sigma coordinate ocean models. *J. Atmos. Oceanic Technol.*, **11**, 1126–1134.
- Olson, D. B., and R. H. Evans, 1986: Rings of the Agulhas. *Deep-Sea Res.*, **33**, 27–42.
- Ou, H. W., and W. P. M. de Ruijter, 1986: Separation of an inertial boundary current from an irregular coastline. *J. Phys. Oceanogr.*, **16**, 280–289.
- Quartly, G. D., and M. A. Srokosz, 1993: Seasonal variations in the region of the Agulhas Retroflexion: Studies with Geosat and FRAM. *J. Phys. Oceanogr.*, **23**, 2107–2124.
- Warren, B. A., 1963: Topographic influences on the path of the Gulf Stream. *Tellus*, **15**, 167–183.